Polymer Journal, Vol. 39, No. 5, pp. 478–487 (2007)

Effect of Structure of Bridging Group on Curing and Properties of Bisphenol-A Based Novolac Epoxy Resins

Guoyuan PAN,[1] Zhongjie DU,[1] Chen ZHANG,[1] Congju LI,[2]
Xiaoping YANG,[1] and Hangquan LI[1,†]

[1]*The Key Laboratory of Beijing City on Preparation and Processing of Novel Polymer Materials, Beijing University of Chemical Technology, Beijing 100029, P. R. China*
[2]*Beijing Key Laboratory of Clothing Material R&D and Assessment, Beijing Institute of Clothing Technology, Beijing 100029, P. R. China*

(Received December 22, 2006; Accepted February 28, 2007; Published April 9, 2007)

ABSTRACT: Three bisphenol-A based novolac epoxy resins with different bridging groups: methylene, methine-phenyl and methine-naphthyl, respectively, between bisphenol-A phenyl rings were prepared to study the effect of structure of bridging group on curing and properties of the epoxy resins. The structures of the obtained epoxy resins were characterized using FT-IR and ^{1}H NMR spectra, the molecular weight and polydispersity index were determined using GPC. The effect of bridging groups on the curing kinetics, thermal mechanical properties, thermal stability, and moisture resistance of the synthesized epoxy resins cured with 4,4′-diaminodiphenyl sulphone (DDS) were investigated by dynamic differential scanning calorimetry, dynamic mechanical analysis, thermogravimetric analysis, X-ray diffraction and moisture absorption measurement. It was concluded that the methylene-bridged epoxy resin possessed the highest curing reaction reactivity toward DDS and the methine-naphthyl-bridged epoxy network possessed the highest storage modulus, glass transition temperatures, thermal stability, and moisture resistance.
[doi:10.1295/polymj.PJ2006201]
KEY WORDS Bisphenol-A / 1-Naphthaldehyde / Benzaldehyde / Bridging Group /

Epoxy resin has been utilized in many applications such as surface coatings, structural adhesives, printed circuit board, insulation materials for electronic devices, and advanced composites matrices due to its good thermal and dimensional stability, excellent chemical and corrosion resistance, and superior mechanical and electrical properties, in addition to ease of handling and processabilities. However, in high-tech applications lower thermal expansion, higher toughness, better heat and moisture resistance were required.[1] For this reason, much work has been continuously directed toward improving their thermal and physical properties by modifications of epoxy resins, in both backbone and pendant groups.[2–5]

Several approaches were adopted to enhance the heat resistance of epoxy resins with increasing cross-link density or introducing bulky structures such as biphenyl or naphthalene.[6–8] The introduction of naphthalene moiety is expected to greatly improve the thermal property and moisture resistance owing to its excellent rigidity, facile packing of molecules and significant degree of hydrophobicity.[9–14] Many studies reported that epoxy resin showed remarkably higher glass transition temperature (T_g), higher thermal stability, higher flexural modulus, better moisture resistance, lower coefficient of thermal expansion when stiff naphthalene was inserted or appended by chemical modification.[15–18] In order to design and develop more novel epoxy resins with higher thermal and mechanical properties to meet the application need, the deeply understanding the effect of the molecular structure of materials on curing behavior, chemical and physical properties of epoxy resin was increasingly more important, because it can predict the end product properties of the new materials and provide a guide for the development process and speed up the development cycle. Varley *et al.* utilized the relationship between the structure and properties as a tool, and formulated high-performance epoxy-amine networks.[19,20] Investigation into the effect of starting materials with analogous molecular structure on properties of the resulting polymer network constituted an important method to understand the mechanism, especially the effect of the molecular structure with bridging group on the properties of epoxy network.[21,22] What's more, some researchers reported the effect of bridging group of curing agent on the curing behavior and properties of epoxy resin system.[23,24] The results also showed that the reactivity and physical properties of the epoxy-amine system depended on the structure of the aromatic amines. However, so far there have been no reports on the effect of bridging groups on the curing kinetics and properties of modified bisphenol-A epoxy resins.

†To whom correspondence should be addressed (Tel: +81-010-64445339, Fax: +81-42-64428804, E-mail: Duzj@mail.buct.edu.cn).

In this study, three bisphenol-A based epoxy resins with different size and structure of methylene, methine-phenyl and methine-naphthyl bridging groups were prepared to study the effect of structure of bridging groups on curing and properties of epoxy resins. For this purpose, the three epoxy resins were synthesized *via* condensation of bisphenol-A with formaldehyde, benzaldehyde, 1-naphthaldehyde, respectively, followed by epoxidation with excess epichlorohydrin. The curing kinetics of the synthesized epoxy resins toward 4,4′-diaminodiphenyl sulphone and the properties of the result polymer network such as thermal mechanical properties, thermal stability and moisture resistance were characterized by differential scanning calorimetry, dynamic mechanic analysis, thermogravimetric analysis, X-ray diffraction and moisture resistance measurement.

EXPERIMENTAL

Materials

Epichlorohydrin (ECH), isopropanol, sodium hydroxide and methyl isobutyl ketone (MIBK) were analytical grade, obtained from Beijing Chemical Co., China, and were furtherly purified prior to use. Unless otherwise noted, all other reagents and chemicals were purchased from commercial suppliers and used without further purifications.

Synthesis of Bisphenol-A Based Novolac Resins[25–27]

A typical preparation was as follows. A 200 mL methyl isobutyl ketone (MIBK) solution containing 68.4 g bisphenol-A (BPA, 0.3 mol) and 1.43 g *p*-toluene sulfonic acid (PTSA, 0.0075 mol) was added to 500 mL four-neck round-bottom flask, equipped with a heating mantle, mechanical stirrer, thermocouple, temperature controller, and a Dean-Stark trap with a reflux condenser. After purging with nitrogen for 10 min, the solution was heated to 100 °C with stirring. A 0.2 mol 1-naphthaldehyde was added dropwise to the solution for about 1 h. Subsequently, the temperature of the flask was kept at 120 °C for 5 h allowing the reaction to occur. Water generated during the reaction was removed *via* azeotropic distillation with MIBK. The condensing of preparing bisphenol-A based novolac resin is reversible, for this reason, the azeotropic distillation method was exclusively utilized in this work.

Subsequently, the above solution was washed with deionized water until it became neutral. The solution was finally evaporated at 180 °C under reduced pressure to remove the unreacted 1-naphthaldehyde and solvent. The remained solid product was washed with a mixture of water/methanol (68/32 v/v) several times to remove the unreacted BPA. A red brown solid product was obtained after vacuum-drying which was denoted as I_c.

Bisphenol-A-formaldehyde novolac resin and bisphenol-A-benzaldehyde novolac resin were synthesized according to the method for synthesis of I_c and were denoted as I_a and I_b, respectively. Figure 1 shows the syntheses of bisphenol-A based novolac resins (I_a, I_b and I_c).

Synthesis of Bisphenol-A Based Novolac Epoxy Resins

A typical preparation was as follows. A 0.15 equivalent of the above synthesized novolac resin based on bisphenol A (I_c) and 3 mol of epichlorohydrin (ECH), 50 g of isopropanol (IPA) were added to a 500 mL four-neck round-bottom flask. After thoroughly mixed at room temperature, the mixture was heated to 70 °C. Subsequently, 32 g of 20 wt % aqueous sodium hydroxide solution was introduced dropwise to the solution with stirring over 1 h. The system was maintained at 70 °C for additional 4 h, and the bottom brine layer was removed by siphoning. The remaining was further reacted with 20 wt % aqueous NaOH 16 g at 70 °C for 1 h. Finally, the product in the flask was washed several times with deionized water to remove the residual sodium chloride, and the excess ECH was thereafter evaporated under a reduced pressure to obtain a light brown-colored solid product denoted as II_c. The corresponding epoxy resins II_a and II_b were obtained from resins I_a and I_b, respectively. Figure 2 shows the syntheses of bisphenol-A based novolac epoxy resins (II_a, II_b, and II_c).

Curing of Bisphenol-A Based Novolac Epoxy Resins

A mixture of bisphenol-A based novolac epoxy resin 5 g and curing agents (DDS) in a molar ratio of 1:1 were dissolved in 40 mL acetone at room temperature and then acetone was evaporated under vacuum. The cured epoxy resins were obtained by mixing the reactant compositions homogeneously at 120 °C, and subsequently cured at 160 °C for 2 h, followed by curing at 200 °C for 10 h, finally postcured at 220 °C for 2 h.

Characterization

FT-IR spectra were recorded using a Nexus 670 infrared spectrometer in the range of 4000–400 cm^{-1} on the KBr pellets.

With deuterated acetone solvent, ^1H nuclear magnetic resonance (^1H NMR) spectra were recorded on a Bruker AV-600 NMR, and tetramethylsilane was used as the internal standard. The operating parameters for ^1H NMR were as follows: sweep width: 600 MHz; pulse width: 5.80 μs; number of scans: 16.

Gel permeation chromatography (GPC) was performed using PE series 200 equipped with polystyrene

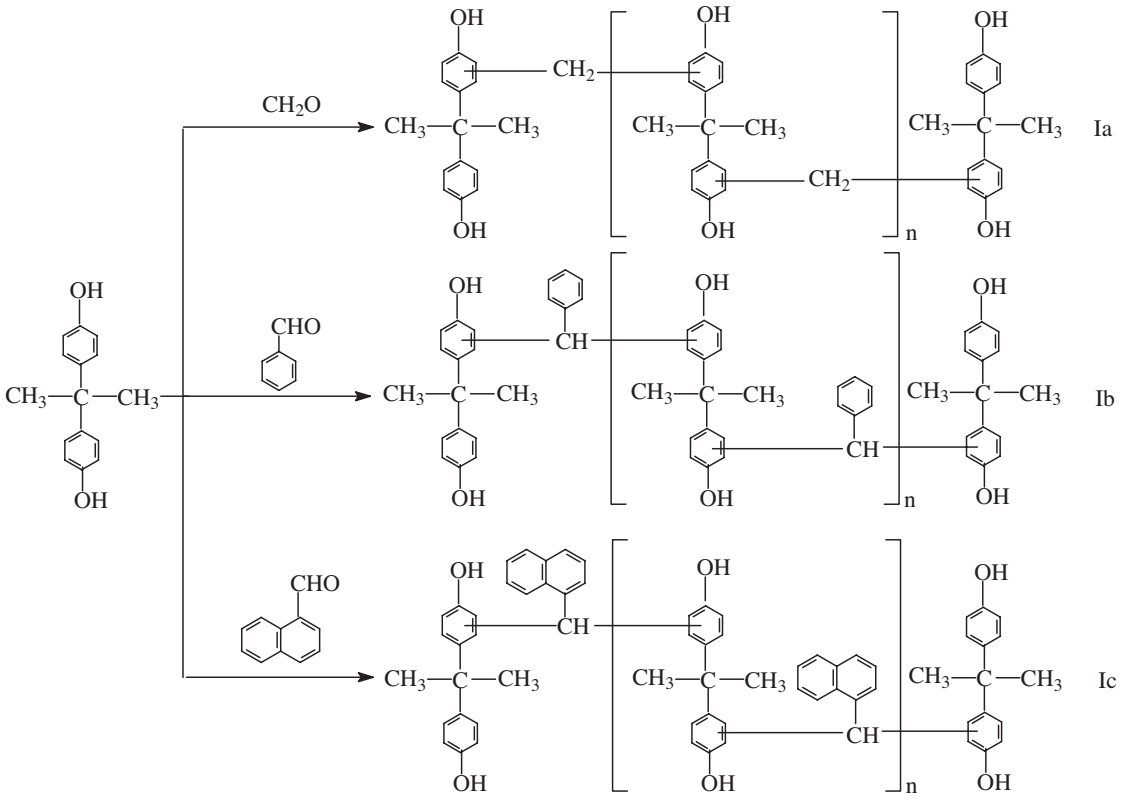

Figure 1. Syntheses of bisphenol-A based novolac resins. (The mole ratio between bisphenol-A and formaldehyde, benzaldehyde, naphthaldehyde was 3:2).

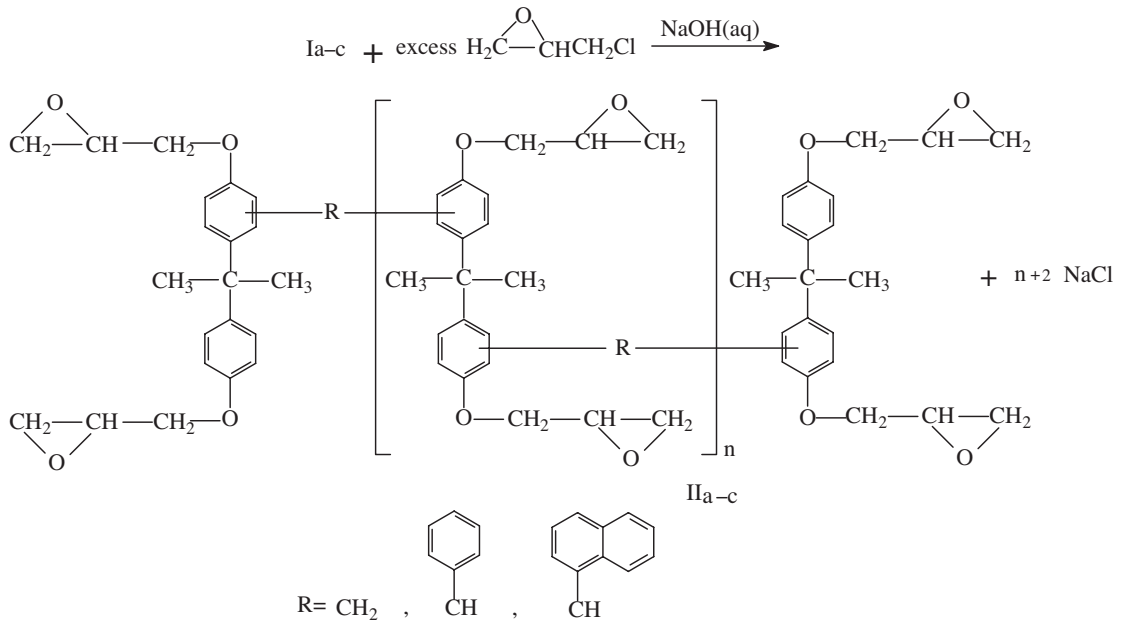

Figure 2. Syntheses of bisphenol-A based novolac epoxy resins.

gel columns and a UV detector at 30 °C at 1 mL/min flow rate.

The epoxy equivalent weights (EEWs) of epoxy resin were determined by the hydrochloric acid-acetone titration.

Differential scanning calorimetry (DSC) were performed using a Shimadzu DSC-41 differential scanning calorimeter by dynamic temperature scan experiments at 5, 10, 15 and 20 °C/min in nitrogen flow.

Dynamic viscoelastic properties were measured using an American Rheometric Scientific DMTA-V thermal analysis system, with DMA mode between

Table I. Average molecular weights and molecular polydispersity index (PID) of bisphenol-A based novolac resins and novolac epoxy resins and their EEWs

Sample code	M_n	M_w	PID (M_w/M_n)	EEW
I_a	750	1340	1.79	—
II_a	890	1770	1.99	200
I_b	780	1690	2.17	—
II_b	950	2110	2.22	238
I_c	810	1570	1.94	—
II_c	960	2220	2.31	263

50 °C and 300 °C, with a heating rate of 5 °C/min at a frequency of 1 Hz under nitrogen atmosphere. The temperature/time scan in a three-point bending mode was chosen and the dimension of the specimen was 30 mm × 5 mm × 2 mm to determine the elastic modulus (E') and mechanical loss factor ($\tan\delta$).

The thermogravimetric analysis (TGA) was performed by simultaneous analyzer NETZSCH STA 449C TG-DSC at a heating rate of 10 °C/min under nitrogen atmosphere at 10 mL/min.

Wide-angle X-ray diffraction patterns (WAXD) were obtained uisng a diffractometer Rigaku D/max-2400 at room temperature using copper filtered Cu Kα radiation (40 KV, 200 mA).

The moisture absorption was determined by placing preweighed 1 mm thick × 50 mm diameter cured disks in boiling water for 72 h to determine the weight gaining.

RESULTS AND DISCUSSION

Characterization of Bisphenol-A Based Novolac Resins and Epoxy Resins

Average molecular weights for three type of bisphenol-A based navolac resins and epoxy resins were listed in Table I, molecular polydispersity index (PDI) and epoxy equivalent weights (EEWs) were also shown. The size of bridging groups increased, the EEWs of epoxy resins increased and thus the crosslinking density of corresponding cured epoxy resins decreased. The effect of EEWs on the properties of cured epoxy resins would be discussed later.

Figure 3(a)–(c) show the FT-IR spectra of bisphenol-A based novolac resins (I_a, I_b, and I_c), respectively. For I_a, the reaction between BPA and formaldehyde was confirmed by the disappearance of the C=O stretch absorption peak at 1640 cm^{-1}, and the appearance of strong broad characteristic absorption peak of phenolic OH stretching vibration at 3342 cm^{-1} (trace a). In the case of I_b, the reaction between BPA and benzaldehyde was approved by the disappearance of the C=O stretch absorption peak at 1702 cm^{-1}, and the appearance of strong broad characteristic absorption peak of phenolic OH stretching vibration at 3359 cm^{-1} (trace b). As far as I_c was concerned, the reaction between BPA and 1-naphthaldehyde was characterized by the disappearance of the C=O stretch absorption peak at 1689 cm^{-1}, the appearance of characteristic absorption peak of α-naphthalene out-of-plane deformation at 776 cm^{-1} and strong broad characteristic absorption peak of phenolic OH stretching vibration at 3406 cm^{-1} (trace c). In the spectra, the strong broad absorption bands in the region 3500–3200 cm^{-1} were assigned to the inter- and intra-molecular hydrogen band phenolic OH stretching vibration (Figure 3(a)–(c)).[28]

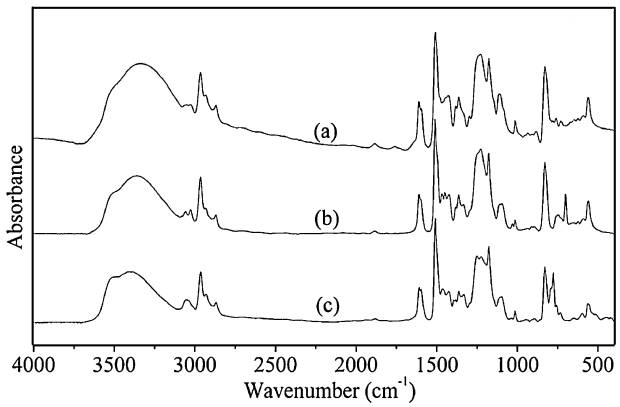

Figure 3. FT-IR spectra of bisphenol-A based novolac resins (a) I_a; (b) I_b and (c) I_c.

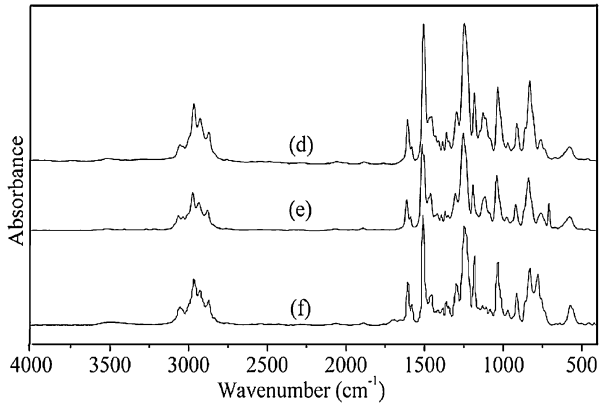

Figure 4. FT-IR spectra of bisphenol-A based novolac epoxy resins (d) II_a; (e) II_b and (f) II_c.

Figure 4(d)–(f) show the FT-IR spectra of biephenol A based novolac epoxy resins (II_a, II_b, and II_c), respectively. The disappearance of broad phenolic OH stretching vibration bands in the region 3500–3200 cm^{-1} (Figure 3(a)–(c)) with the appearance of new strong bands at 840 and 914 cm^{-1} (Figure 4(d)–(f)) due to the symmetrical and asymmetrical stretching modes of epoxy group,[29] respectively, indicated the completion of etherification of phenolic hydroxyl.

Figure 5(a)–(c) show the ^1H NMR spectra of bi-

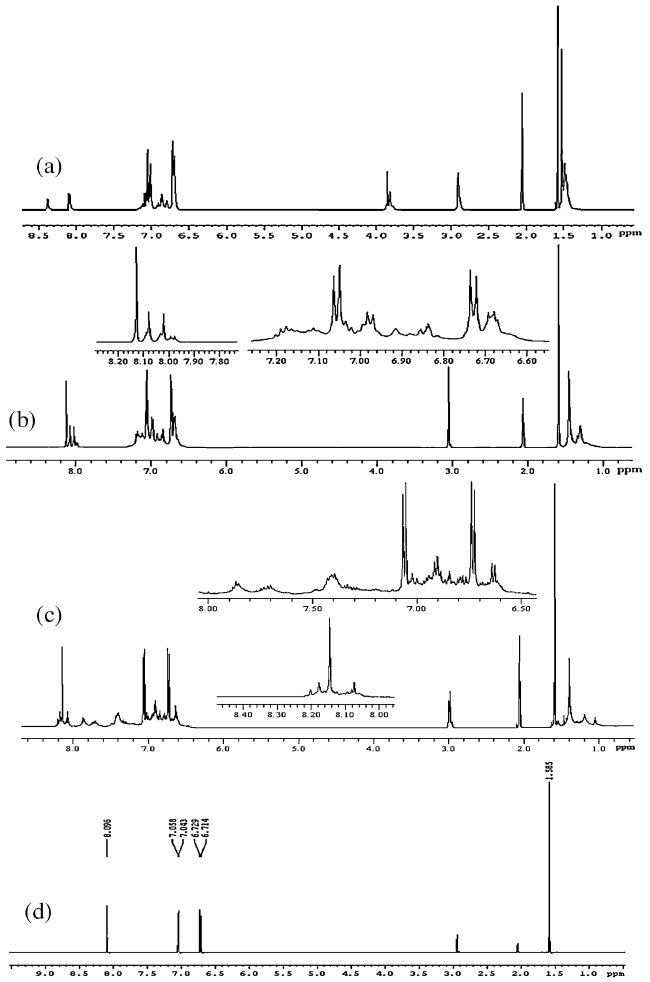

Figure 5. ^{1}H NMR spectra of (a) I_a, (b) I_b, (c) I_c and (d) BPA in acetone-d_6.

sphenol-A based novolac epoxy resins (I_a, I_b, and I_c) in acetone-d_6, respectively. For I_a, the multiplet peaks at 1.491–1.585 ppm, 3.817–3.846 ppm, 6.692–7.058 ppm, and 8.081–8.684 ppm (Figure 5(a)) can be assigned to methyl, methylene bridges, aromatic, and hydroxyl protons, respectively. Concerning I_b, single peak at 1.595 ppm, multiplet peaks at 1.255–1.459 ppm, 6.685–7.196 ppm, and 8.020–8.128 ppm (Figure 5(b)) can be attributed to methyl, methine bridges (–CH–C_6H_5), aromatic, and hydroxyl protons, respectively. For I_c, multiplet peaks at 1.202–1.411 ppm, 1.556–1.633 ppm, 6.627–7.067 ppm, 7.289–7.880 ppm, and 8.024–8.186 ppm (Figure 5(c)) can be due to methine bridges (–CH–$C_{10}H_7$), methyl, aromatic (–C_6H_5), aromatic (–$C_{10}H_7$), and hydroxyl protons, respectively. Methylene, methine (–CH–C_6H_5), and methine (–CH–$C_{10}H_7$) bridges are the characteristic structures of I_a, I_b, and I_c, respectively, which can be obviously seen by comparing with the ^{1}H NMR spectrum of BPA (Figure 5(d)). In addition, two multiplet peaks corresponding to the aromatic protons on the phenol ring at 6.692–6.728 ppm (ortho to the phenolic hydroxyl group) and 7.016–7.058 ppm (meta to the phenolic hydroxyl group) were observed symmetrical about a central point, this was because that BPA is a para-substituted aromatic compounds in which two substitutents differ from each other in electronic effects. However, compared with the ^{1}H NMR spectrum of BPA, the symmetrical patterns became complex and some split peaks appear between 6.728–7.016 ppm, which was assigned to the effect of the methylene, methine (–CH–C_6H_5), and methine (–CH–$C_{10}H_7$) bridges bonding to the BPA phenyl rings. In fact, the eight active positions on BPA for the methylene, methine (–CH–C_6H_5), and methine (–CH–$C_{10}H_7$) bridges to bond to the BPA phenyl rings can be categorized into two kinds, ortho and meta positions. The two kinds of positions appeared to possess the same bonding chance to the methylene, methine (–CH–C_6H_5), and methine (–CH–$C_{10}H_7$) bridges, which was indicated by the ratio of the peak areas for the two kinds of aromatic protons. Moreover, the ratios of area integrations for peaks (ph–CH_2–Ph/aromatic protons/Ph–C–CH_3) (Figure 5(a)), (ph–CH(–C_6H_5)–Ph/aromatic protons/Ph–C–CH_3) (Figure 5(b)), and (ph–CH(–$C_{10}H_7$)–Ph/aromatic protons/Ph–C–CH_3) (Figure 5(c)) were consistent with the proposed statistical structures of I_a, I_b, and I_c, respectively, shown in Figure 1.

Effect of the Structure of Epoxy Resins on Thermal Curing Reaction and Kinetics

Figure 6(a)–(c) show the DSC traces of the cured epoxy resins of II_a, II_b, and II_c, respectively, with DDS. The temperature of the deviation from the baseline (T_i), the exotherm peak position (T_p), the temperature of completion of the exotherm (T_f), and the total reaction heat of curing (ΔH) were listed in Table II. The values of T_i, T_p, T_f and ΔH inecreased with increasing heating rate. The value of T_i depended on the reactivity of the epoxy resins toward DDS, and increasing in the order of $II_a < II_b < II_c$. The higher the value of T_i, the lower the reactivity of epoxy resin, therefore, the reactivity of II_c was lowest toward DDS.

In order to evaluate the curing reaction kinetic parameters, two multiple-heating-rate methods proposed by Flynn-Wall-Ozawa and that by Kissinger were used.[30–32] The above two methods assume that the exotherm peak temperature α_p was constant and was independent of the heating rate.[33,34] This made the *nth* order and the autocatalytic reactions equally effective. For the Kissinger method, the maximum reaction rate occurs at peak temperatures, where $d^2\alpha/dt^2 = 0$, in this way, it can be expressed as

$$\ln\left(\frac{\beta}{T_p^2}\right) = \ln\left(\frac{AR}{E_a}\right) - \frac{E_a}{RT_p} \qquad (1)$$

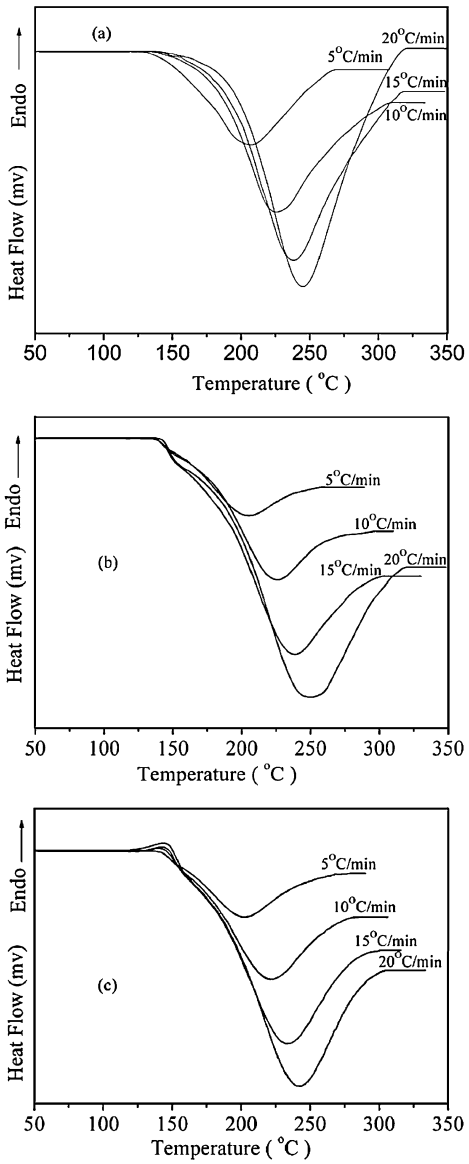

Figure 6. DSC thermograms for (a) II_a/DDS, (b) II_b/DDS and (c) II_c/DDS systems at different heating rates.

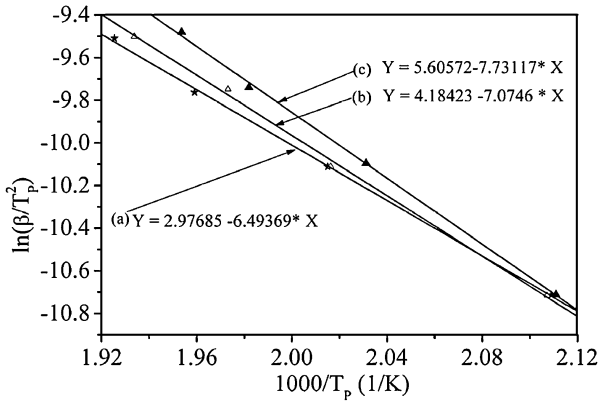

Figure 7. Plots for determination the activation energy of the curing reaction by Kissinger method: (a) II_a/DDS; (b) II_b/DDS and (c) II_c/DDS.

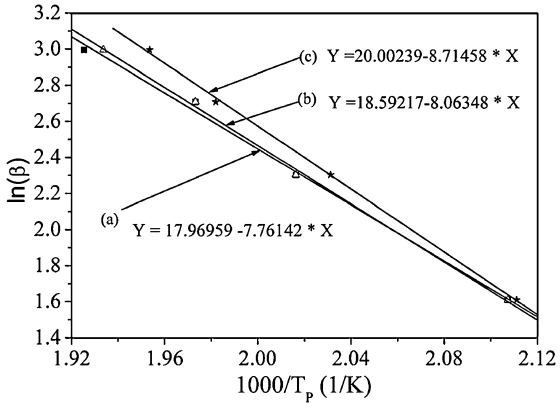

Figure 8. Plots for determination the activation energy of the curing reaction by Ozawa method: (a) II_a/DDS; (b) II_b/DDS and (c) II_c/DDS.

where T_p is the exotherm peak temperature, β is the linear heating rate, A is the frequency factor, E_a is the activation energy and R is the universal gas constant. Therefore, E_a can be obtained by plotting $\ln(\beta/T_p^2)$ *vs* T_p^{-1}, as displayed in Figure 7.

Based on eq 1, the frequency factor A can be obtained:

$$A = \beta E_a \exp(E_a/RT_p)/RT_p^2 \tag{2}$$

The Flynn-Wall-Ozawa method yields a simple relationship between the activation energy, the heating rate, and iso-conversion temperature. It assumed that the degree of conversion at peak temperatures for different heating rates was constant, this giving the activation energy as:

$$E_a = -\frac{R}{0.4567}\frac{\mathrm{d}\log\beta}{\mathrm{d}(1/T_i)} = -\frac{R}{1.052}\frac{\mathrm{d}\ln\beta}{\mathrm{d}(1/T_i)} \tag{3}$$

where T_i is the iso-conversion temperature and other parameters are the same as described above. Plotting $\ln\beta$ *vs.* $1/T_p$, as shown in Figure 8, the activation energy can be obtained from the slope. The advantage here is that the activation energy can be measured over the entire course of the reaction.

All the dynamic cure parameters of various epoxy systems calculated from above equations are summarized in Table II. One may notice that although the activation energy values obtained from the two models are different, they are in the order of II_a/DDS<II_b/DDS<II_c/DDS, consistent with that for the reactivity. The values of A, which account for the differences in stereo, electronics, collision factors is also in the order as activation energy: II_a>II_b>II_c.

This result may be attributed to difference of the steric hindrance of the bridging group in II_a, II_b and II_c. For II_c, the methane-naphthyl linkage which pos-

Table II. Curing characteristics of the samples evaluated with DSC thermograms

Sample code	Heating rate (°C/min)	T_i (°C)	T_p (°C)	T_f (°C)	ΔH (J/g)	E_a (KJ/mol) Kissinger	E_a (KJ/mol) Ozawa	ln(A) min^{-1}
II_a/DDS	5	116.5	201.2	276.9	176.3	54.83	61.34	11.99
	10	119.8	223.3	307.2	265.9			11.97
	15	123.5	237.5	319.8	284.4			11.95
	20	127.8	246.4	321.0	290.5			11.98
II_b/DDS	5	136.3	201.6	258.1	151.9	58.82	63.73	13.06
	10	139.7	223.0	296.7	154.9			13.02
	15	140.6	233.8	301.0	160.3			13.07
	20	141.0	244.1	319.8	186.1			13.04
II_c/DDS	5	137.5	200.7	278.6	198.4	64.28	68.87	14.56
	10	141.9	219.3	294.9	201.4			14.56
	15	144.3	231.6	300.3	203.9			14.54
	20	144.7	238.9	311.6	210.0			14.58

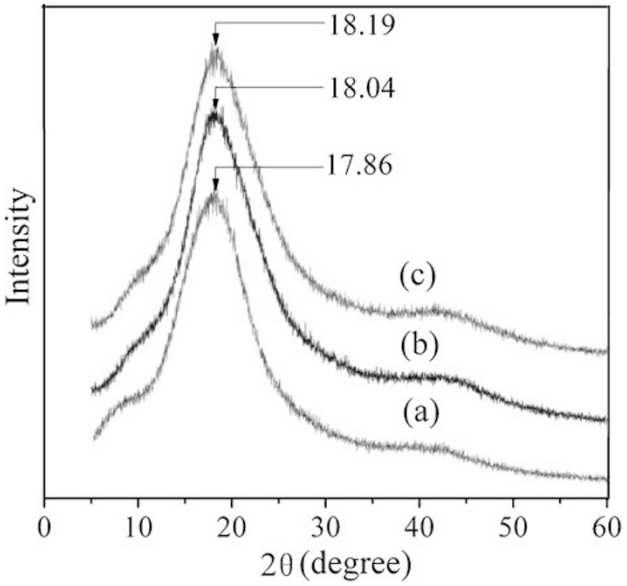

Figure 9. WAXD patterns for cured systems of (a) II_a/DDS; (b) II_b/DDS and (c) II_c/DDS.

sessed the lowest flexibility and largest size reduced the molecular mobility and depressed the reactivity of reactive site to the greatest extent. The reactions between the bridging groups and DDS are mainly the addition of amine to the epoxy group, which are generally related to the steric, inductive and resonance nature of monomer structure. In the precursors II_a, II_b and II_c, the reactive sites are separated by almost the same distance, however, the EEW of II_c is the highest, as a consequence, its functional group spatial density is the lowest and the molecules appear to be the most immobile during reaction.

Wide-Angle X-Ray Diffraction Patterns

Figure 9 shows the room temperature wide-angle X-ray diffraction diagrams for cured systems of II_a/DDS, II_b/DDS, and II_c/DDS. The absence of noticeable diffractions primarily indicated that the cured systems were amorphous. However, the difference in the center of the three broad arches suggested that the packing was somewhat different for three systems. Calculated from the location of the peaks, the average inter-segment distance in II_a/DDS, II_b/DDS, and II_c/DDS systems was 5.02 Å, 4.91 Å, and 4.87 Å, respectively, which suggested that the last system was most densely compacted.

Effect of the Structure of Epoxy Resins on Cured Resins Mechanical and Thermal Properties

Figure 10(a) and (b) show the dependence of storage modulus (E's) and tan δ of the cured systems, respectively. The methine-naphthyl-bridged epoxy network possessed highest E' in glassy region, and the methine-phenyl-bridged epoxy network being the second. There were mainly two factors which controlled the E's of the epoxy networks. One was the crosslinking density of epoxy networks, the other was the size of bridging groups. One can find from Table I, the EEWs of the epoxy resins increase in the order of $II_a < II_b < II_c$, the higher the EEW, the lower the crosslinking density of the epoxy network. An decrease of the crosslinking density can increase the chain mobility and, consequently, decreases the values of the E's.[35] In the other hand, the size of the bridging groups increase in the order of $II_a < II_b < II_c$. On above discussion, an increase in the size of the bridging groups between two bridging points can increase the average inter-segment distance, thus increase the steric hindrance, as a result, lower the movement of the molecular chain and increase the values of the E's. The results indicated that the effect of size of bridging groups on the chain mobility prevailed over that of the crosslinking density. Therefore, the E's of epoxy network can be elevated drastically by the introducing some bulky rigid group into the backbone of monomer.

The glass transition temperature was indicated by

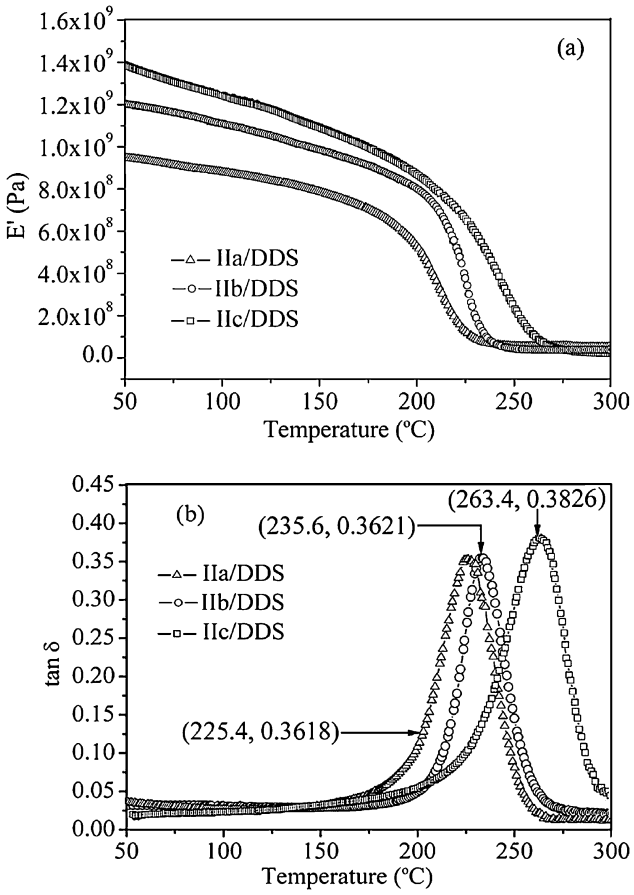

Figure 10. Temperature dependences of (a) storage modulus E' and (b) tan δ for cured II_a/DDS, II_b/DDS and II_c/DDS.

the peak of tan δ. Again, one may notice that the methine-naphthyl-bridged and methine-phenyl-bridged epoxy networks exhibited higher T_gs than that of methylene-bridged epoxy network. This may result from the rigidity imparted by the methine-naphthy and methane-phenyl groups to the crosslinked network, which restrained the movements of the polymer segments, and revealed that T_g was influenced more strongly by the backbone rigidity of epoxy, *i.e.*, was affected more by molecular mobility than by crosslinking density, therefore, it is possible to design epoxy systems that exhibit high T_g, high modulus.

Figure 11 presents the TGA and DTG traces of the cured systems: (a) II_a/DDS; (b) II_b/DDS and (c) II_c/DDS under nitrogen atmosphere, and the TGA data for various polymers are collected in Table III. As depicted in Table III, by comparing the T_5, T_{10} and T_{max}, one can find that II_b and II_c networks demonstrated better resistance to thermally degradation than II_a network. This result probably related to the introduction of more thermal resistance aromatic bridging groups. The percent char yield for cured systems at 600 °C and 800 °C decreased in the order of $II_c > II_b > II_a$. This may be proposed that, for cured systems II_b/DDS and II_c/DDS, because of the incorporation of aromatic

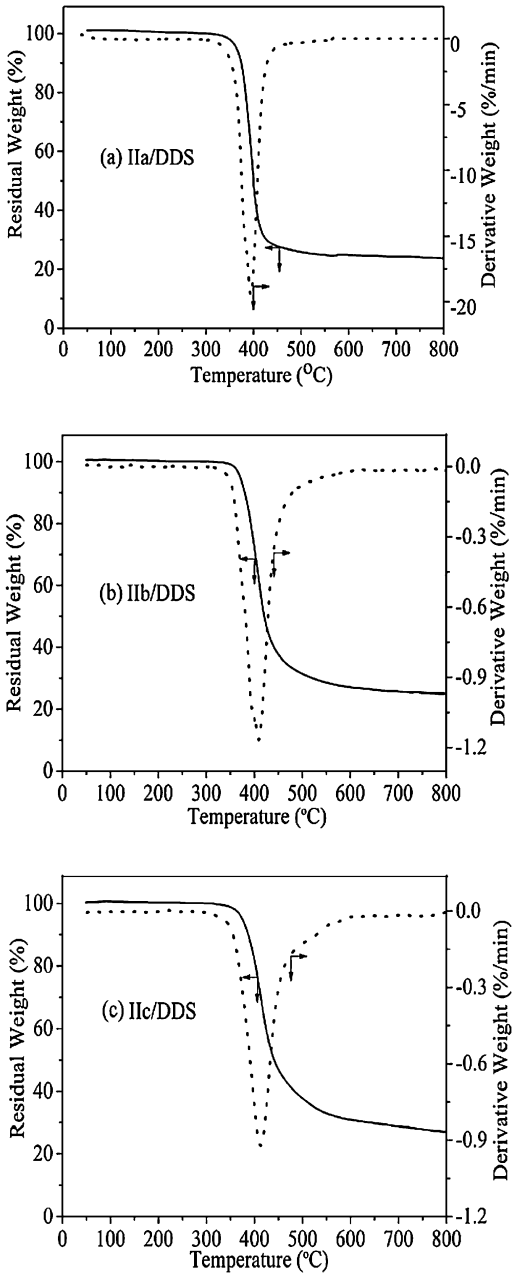

Figure 11. TGA and DTG traces for DDS cured epoxy polymers under nitrogen atmosphere.

Table III. Thermogravimetric analysis of cured polymers

Sample code	[a]T_5 (°C)	[b]T_{10} (°C)	[c]T_{max} (°C)	Char yield at 600 °C (%)	Char yield at 800 °C (%)
II_a/DDS	355	374	397	24.82	23.67
II_b/DDS	370	380	409	27.03	24.97
II_c/DDS	375	387	412	30.88	27.10

[a]T_5, temperature of 5% weight loss. [b]T_{10}, temperature of 10% weight loss. [c]T_{max}, temperature of maximum rate of weight loss under nitrogen atmosphere.

Table IV. Moisture absorption of cured epoxy resins

Sample code	Water absorption gains (wt %)				
	12 h	24 h	36 h	48 h	72 h
II_a/DDS	1.547	2.129	2.258	2.336	2.427
II_b/DDS	1.521	2.072	2.157	2.287	2.365
II_c/DDS	1.474	2.045	2.123	2.268	2.308

bridging groups, the formation of char is facilitated, and for the latter, the higher percent of aromatic moieties was introduced.

Effect of the Structure of Epoxy Resins on the Moisture Absorption of Cured Resins

In the practical using, absorbed moisture was found to plasticize the epoxy resin,[36] causing a lowering of the T_g and in turn affecting mechanical properties,[37–39] therefore, has attracted many studies.[40–42] The moisture absorption measurement is shown in Table IV. It showed that all cured aromatic bridging group containing epoxy resins (II_b and II_c) had better moisture resistance than that of aliphatic bridging group containing epoxy resin (II_a). The epoxy networks with aromatic bridging groups possessed smaller average inter-segment distance, indicated that they had smaller free volume, this can lead to a lower moisture absorption. Moreover, during the curing process, –OH groups were generated *via* ring opening of epoxy groups.[43–46] With the EEW of epoxy resin increasing, the ring opening of epoxy reduced, thus less polar –OH groups were produced leading to a higher hydrophobicity of the cured system.

CONCLUSIONS

The effect of the bridging groups on the thermal curing behavior of bisphenol-A based epoxy resins with DDS was investigated, the activation energy value obtained from Kissinger and Ozawa method was fairly close and both in the trend $II_a<II_b<II_c$, the same with A, this revealed that the steric hindrance of the epoxy resin systems in the order $II_a<II_b<II_c$, in other word, the bigger the size of bridging group, the higher the rigidity of epoxy resin. The methine-naphthyl-bridged epoxy network possessed the highest storage modulus, glass transition temperatures, thermal stability, and moisture resistance. These excellent overall performances for II_c enable them a promising candidate to substitute II_a in composite matrix and printed wiring boards, and integrated circuit encapsulations.

Acknowledgment. This work was supported by National Natural Science Foundation of China (No. 50503004).

REFERENCES

1. A. Igarashi, T. Terasawa, M. Kanie, T. Yamanobe, and T. Komoto, *Polym. J.*, **37**, 522 (2005).
2. C. B. Bucknall and A. H. Gillbert, *Polymer*, **30**, 213 (1989).
3. C. S. Wang and M. C. Lee, *Polymer*, **41**, 3631 (2000).
4. S. P. Rwei, C. Y. Cheng, G. S. Liou, and K. C. Cheng, *Polym. Eng. Sci.*, **45**, 478 (2005).
5. H. Okamura, K. Shin, and M. Shirai, *Polym. J.*, **38**, 1237 (2006).
6. C. S. Wang and M. C. Lee, *J. Appl. Polym. Sci.*, **73**, 1611 (1997).
7. A. Matsumoto, K. Hasegawa, and A. Fukuda, *Polym. Int.*, **30**, 65 (1993).
8. K. Ohta, W. Kosaka, and K. Yanagisawa, Eur. Patent 0 428 871 A2 (1991).
9. C. S. Wang and M. C. Lee, *J. Appl. Polym. Sci.*, **70**, 1907 (1998).
10. C. P. Yang and W. T. Chen, *J. Polym. Sci., Part A: Polym. Chem.*, **31**, 2799 (1993).
11. J. Y. Lee and J. Jang, *J. Polym. Sci., Part A: Polym. Chem.*, **37**, 419 (1999).
12. C. S. Wang, T. S. Leu, and K. R. Hsu, *Polymer*, **39**, 2921 (1998).
13. L. Callau, J. A. Reina, A. Mantecon, M. Tessier, and N. Spassky, *Macromolecules*, **32**, 7790 (1999).
14. K. J. Patel, K. G. Amin, and R. G. Patel, *J. Appl. Polym. Sci.*, **75**, 1345 (2000).
15. K. Xu, M. C. Chen, K. Zhang, and J. W. Hu, *Polymer*, **45**, 1133 (2004).
16. M. Kaji and T. Endo, *J. Polym. Sci., Part A: Polym. Chem.*, **37**, 3063 (1999).
17. T. H. Ho, *Macromol. Mater. Eng.*, **283**, 57 (2000).
18. Y. F. Duann, T. M. Liu, K. C. Cheng, and W. F. Su, *Polym. Degrad. Stab.*, **8**, 305 (2004).
19. R. J. Varley, J. H. Hodgkin, and G. P. Simon, *J. Appl. Polym. Sci.*, **77**, 237 (2000).
20. A. Chateauminois, V. Sauvant, and J. L. Halary, *Polym. Int.*, **52**, 507 (2003).
21. K. Xu, M. C. Chen, X. J. Zhang, and K. Zhang, *Macromol. Chem. Phys.*, **205**, 1559 (2004).
22. J. Y. Lee, J. Jang, S. M. Hong, S. S. Hwang, and K. U. Kim, *Polymer*, **40**, 3197 (1999).
23. P. Jain, V. Choudhary, and I. K. Varma, *Eur. Polym. J.*, **39**, 181 (2003).
24. N. Gupta and I. K. Varma, *J. Appl. Polym. Sci.*, **68**, 1759 (1998).
25. C. Gouri, C. P. Reghunadhan Nair, and R. Ramaswamy, *Polym. Int.*, **50**, 403 (2001).
26. T. H. Ho and C. S. Wang, *J. Appl. Polym. Sci.*, **74**, 1905 (1999).
27. C. H. Lin, J. C. Chiang, and C. H. Wang, *J. Appl. Polym. Sci.*, **88**, 2607 (2003).
28. M. Ayman. N. O. Atta, N. E. Shaker, and Maysour, *Prog. Org. Coat.*, **56**, 100 (2006).
29. R. Arridge and J. Speake, *Polymer*, **13**, 443 (1972).
30. T. Ozawa, *J. Therm. Anal. Calorim.*, **2**, 301 (1970).
31. J. H. Flynn and L. A. Wall, *J. Appl. Polym. Sci.*, **4**, 323

(1966).
32. H. E. Kissinger, *Anal. Chem.*, **29**, 1702 (1957).
33. R. B. Prime, *Polym. Eng. Sci.*, **13**, 365 (1973).
34. M. C. Lu and J. L. Hong, *Polymer*, **35**, 2822 (1994).
35. S. G. Allen, in "Comprehensive Polymer Sciences: the Synthesis, Characterization, Reactions and Applications of Polymers," C. Booth and C. Price, Ed., Pergamon Press, New York, 1989, Vol. 2, p 311.
36. M. C. Lee and N. A. Peppas, *Prog. Polym. Sci.*, **18**, 947 (1993).
37. E. L. Mckague, J. D. Reynolds, and J. E. Halkies, *J. Appl. Polym. Sci.*, **22**, 1643 (1978).
38. J. Mijovic and K. F. Lin, *J. Appl. Polym. Sci.*, **30**, 2527 (1985).
39. P. Musto, L. Mascia, G. Ragosta, G. Scarinzi, and P. Villano, *Polymer*, **41**, 565 (2000).
40. G. Z. Xiao and M. E. R. Shanahan, *Polymer*, **39**, 3253 (1998).
41. E. Boinard, R. A. Pethrick, J. Dazel-Job, and C. J. Macfarlane, *J. Mater. Sci.*, **35**, 1931 (2000).
42. T. Kimura, Y. Nakamoto, and G. Konishi, *Polym. J.*, **38**, 606 (2006).
43. N. Sbirrazzuoli, A. Mititelu-Mija, V. Luc, and C. Alzina, *Thermochim. Acta*, **447**, 167 (2006).
44. A. Catalani and M. G. Bonicelli, *Thermochim. Acta*, **438**, 126 (2005).
45. S. Vyazovkin and N. Sbirrazzuoli, *Macromolecules*, **29**, 1867 (1996).
46. S. Swier, G. V. Assche, W. Vuchelen, and V. M. Bruno, *Macromolecules*, **38**, 2281 (2005).